PHASE-DEPENDENT FINITE DIFFERENCE HEAT TRANSFER ANALYSIS WITH HEAT EXCHANGER APPLICATIONS

An Undergraduate Research Scholars Thesis

by

AUGUSTUS ELLIS, ANTHONY HRESKO, and BLAKE LEIKER

Submitted to the Undergraduate Research Scholars program at
Texas A&M University
in partial fulfillment of the requirements for the designation as an

UNDERGRADUATE RESEARCH SCHOLAR

Approved by Research Advisor: Dr. Jonathan Felts

May 2017

Major: Mechanical Engineering

TABLE OF CONTENTS

ABSTRACT

Phase-Dependent Finite Difference Heat Transfer Analysis with Heat Exchanger Applications

Augustus Ellis, Anthony Hresko, and Blake Leiker
Department of Mechanical Engineering
Texas A&M University

Research Advisor: Dr. Jonathan Felts
Department of Mechanical Engineering
Texas A&M University

The finite difference method, a form of nodal analysis, is a powerful tool for developing accurate models of the changing thermal states of an object. With this method, a body that is too large or too complex for analytical heat transfer analysis can be separated into many smaller subvolumes for which the analytical equations are reasonable to solve. For this project, the goal is to develop a program that uses the finite difference method to model the heat transfer within a body subject to external effects, temperature dependent thermophysical properties, and material phase changes. The specific application that this program will be used for is modeling a simplified phase changing heat exchanger system, allowing for simulations to be run of various heat exchanger geometries and leading to a more optimized heat exchanger design. The program is predominantly written in C++, with MATLAB used for data visualization purposes. A node sensitivity study was also run to validate the stability of the model.

ACKNOWLEDGEMENTS

We would like to thank our research advisor, Dr. Jonathan Felts, for his guidance and support throughout the course of this work.

NOMENCLATURE

PCM	Phase Change Material
k	Thermal Conductivity
c_p	Specific Heat Capacity
T	Temperature
q	Heat

SECTION I

INTRODUCTION

Being able to understand and determine quantitatively the thermal state of an object is essential to properly engineering a design. Unfortunately, analytical solutions to most of these thermal states are difficult and sometimes impossible to obtain. To combat this difficulty, approximate computational methods were developed [1]. One of these computational methods, and the focus of this study, is the finite difference method. It is a type of nodal analysis in which an object is separated into a large number of smaller volumes for which analytical heat transfer solutions can be obtained. These many analytical solutions are then solved simultaneously to obtain the overall thermal state. By using the finite difference method, complex thermal states can be modeled that would otherwise be impractical to calculate analytically [2].

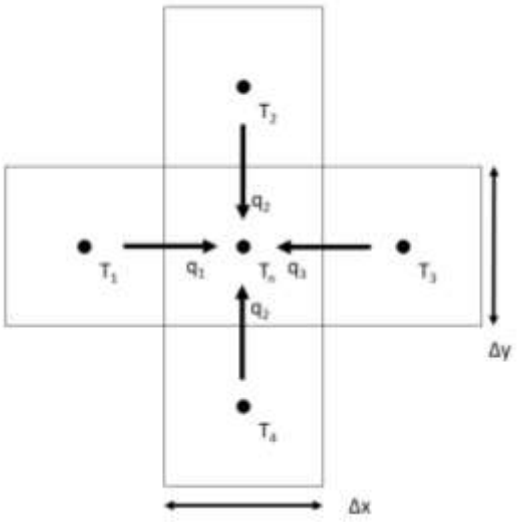

Figure 1. Internal Node Diagram

The diagram in Figure 1 is a common one for simple finite difference methods that consists of a single cubic subvolume and the six (four for two-dimensional), surrounding, cubic

subvolumes. Heat is transferred between the subvolumes via conduction under the assumption of linear temperatures gradients between adjacent nodes. The heat transfer between the central subvolume and the surrounding subvolumes is calculated as shown in Equations 1-4.

$$q_1 = k\Delta y\Delta z(\frac{T_1 - T_n}{\Delta x}) \quad (1)$$

$$q_2 = k\Delta x\Delta z(\frac{T_2 - T_n}{\Delta y}) \quad (2)$$

$$q_3 = k\Delta y\Delta z(\frac{T_3 - T_n}{\Delta x}) \quad (3)$$

$$q_4 = k\Delta x\Delta z(\frac{T_4 - T_n}{\Delta \mathrm{y}}) \quad (4)$$

Combining the four formulas in Equations 1 through 4 using the conservation of energy principle yields Equation 5, which can be used to calculate the thermal gradient in a 2-D system with constant phase and thermal conductivity. This also assumes that the node is a cube and therefore $\Delta x, \Delta y, and\ \Delta z$ are the same size. This is a simple example of applying finite difference methods.

$$k(T_1 - T_n + T_2 - T_n + T_3 - T_n + T_4 - T_n) = \rho c_p \Delta x^2 \frac{dT}{dt} \quad (5)$$

The goal of this research project is to use the above finite difference methods—extended to include multiple material phases and temperature dependent properties [3]—to model the heat flow around and through a phase change heat exchanger [4]. Phase change heat exchangers allow one to work outside of the limit of the exchanger material's heat capacity and to transfer greater amounts of energy as compared to conductive or convective heat exchangers. This additional capability comes from storing energy in the phase transformation itself through latent heat. Future plans to expand upon this project will be to build the modeled heat exchanger to test the efficacy of the model.

SECTION II

METHODS

Finite Difference Modeling and Simulation

The first step of this project was to develop a model and simulation for heat flow through a body. For this simulation, C++ and the finite difference method described in the introduction were used. Since C++ is an object-oriented language, the simulation and its components were implemented as C++ classes: A Node class, a Mesh class, and a Material class. The Mesh class contained a number of instances of the Node class (one for each subvolume) and each instance of the Node class contained a reference to a Material class with the appropriate material properties for that node. At each time step in the simulation, the Mesh class calculates the net amount of heat that should flow into each node, passes this heat to each Node class wherein each node calculates its own change in temperature and state. These temperature changes are then passed to the Material class, which updates the material properties as appropriate. In this fashion, the simulation steps through time.

The simulation process occurs in two distinct cycles: a heating cycle and a cooling cycle. During the heating cycle, the program uses the boundary conditions (bottom surface of the mesh is constant temperature, all other surfaces are adiabatic) to determine the heat input to each node. Within each node, temperature and state are tracked as follows: 1) the node increases in temperature until the material melting temperature is reached, at which point 2) any additional heat is added to the latent heat of that node and the temperature is held constant at that melting temperature, and then 3) once the latent heat of a node reaches the latent heat of fusion for the given material, the program marks the node as liquid and the temperature begins to rise again

based on the input heat. The process is similar for the cooling cycle. The liquid nodes decrease in temperature until reaching the melting point at which the temperature is held constant until all latent heat has been dispersed. At that point, the node is solid again and the temperature begins to drop.

Once the program accurately modeled heat transfer and successfully handled phase changes, the next step was to apply it to the specific materials and geometries. The modeled heat exchanger was separated into a number of repeating units each of which should have similar, if not identical, temperature profiles and phase distributions. That repeating unit can be seen below in Figure 2. It consists of half of a fin, one trough between fins, and half of the next fin. To model that unit, nodes in the grey area were given the material properties of stainless steel and the nodes the blue area were given material properties of the phase change material (PCM). The bottom most row of nodes is set to the temperature of water flowing on the other side of the heat exchanger. The sides can be considered adiabatic because of the symmetry of the repeating unit, and the top will also be considered adiabatic due to the insulating behavior of the plastic covering on that side of the heat exchanger. In addition, the repeating unit has an additional line of temperature symmetry along its centerline. Due to the line of symmetry at the centerline of the unit, only the right half of each repeating unit was simulated.

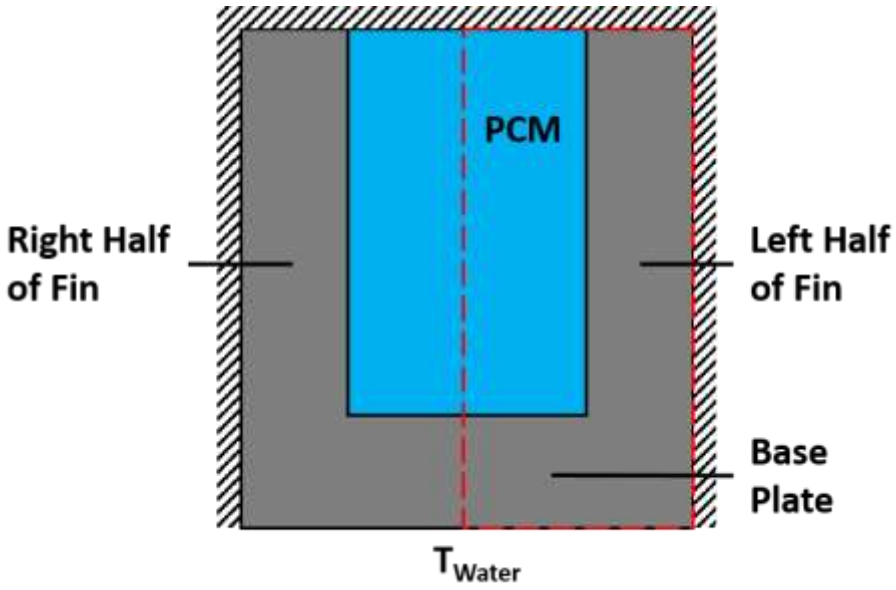

Figure 2. Repeating unit for finite difference simulation.

To determine the most effective heat exchanger geometry, the repeating base unit shown above was simulated for differing configurations of fin and PCM geometry. This consisted of varying the fin height, width, and spacing. This was done in order to determine an optimal geometry. Because the phase change materials used in phase change heat exchangers generally have a low thermal conductivity, phase change heat exchangers are at their most effective when all the PCM changes phase roughly simultaneously. Because of this fact, one method of determining optimum heat exchanger geometry using the finite difference simulation is to calculate the amount of time required for full phase change of the PCM to occur. Once the model was completed and the results were validated, the simulation was iterated through differing fin and PCM geometries to determine the effect on phase change time.

Total phase change time is also dependent on the total volume of PCM within the heat exchanger. Smaller volumes of PCM require less total energy to melt them and thus will generally melt more quickly even in less than optimum fin geometries. Because of this, the PCM melting time was normalized with respect to the total PCM volume within a model heat

exchanger. As this model will eventually be experimentally verified through the testing of PCM, a heat exchanger was fully designed; this volume of PCM within this heat exchanger is what has been used to calculate the ratio of melting time to volume. The heat exchanger plate to be used is shown below in Figure 3 and Figure 4.

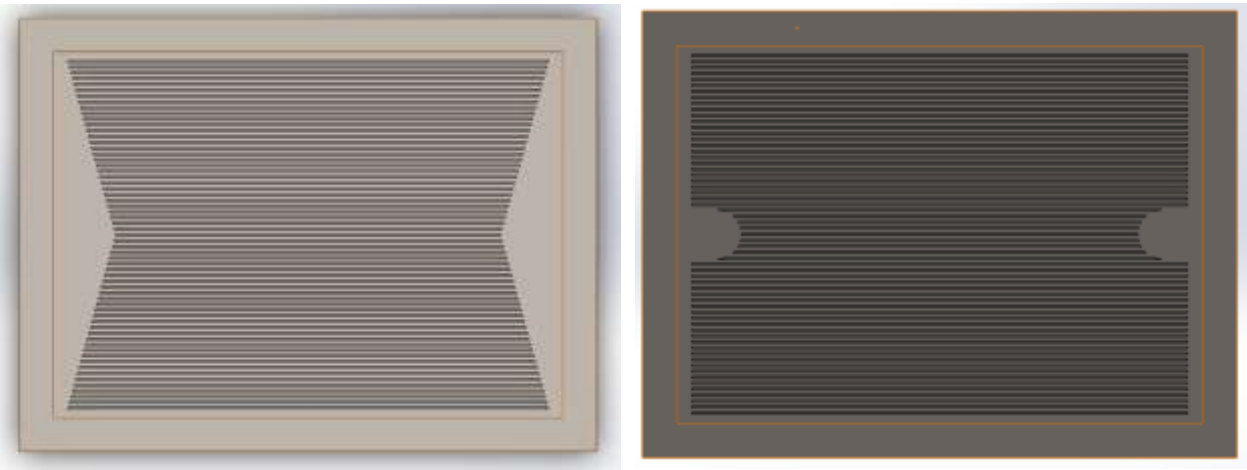

Figure 3. Heat Exchanger Plate, Front and Back Views.

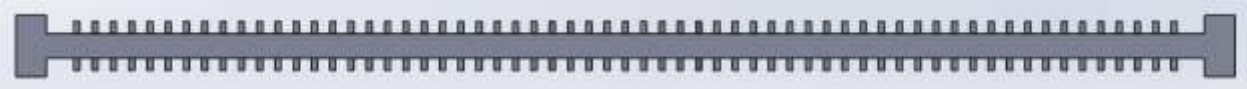

Figure 4. Heat Exchanger Plate, Cross-Sectional View.

The heat exchanger shown has been designed such that water will flow through the fins of one side, either heating or cooling to melt or solidify the PCM on the other side. The fin length is 5 inches, and the length of usable fin space, which is the width of the finned portion of the heat exchanger, is 3.62 inches. These numbers were used in conjunction with various values of fin height, width, and spacing to determine the volume of PCM that will be able to fill between the fins. The PCM will fill these fin gaps, as shown above in Figure 2 through the entire volume of one side of the heat exchanger, shown above in Figure 4. Using these varying values of fin height, width, and spacing, the calculated ratios of melting time to total volume of PCM

within the heat exchanger were analyzed to determine an optimal fin geometry using the aforementioned measure of melting time to total PCM volume.

SECTION III

RESULTS

Modeling and Simulation Results

In order to analyze the results of the finite difference simulation, the temperature of each node at each time step was saved and tracked so that the overall temperature distribution of the modeled base unit could be observed. The results of each time step were placed into videos that allowed for easy viewing of the behavior of the modeled base unit. Figure 5 below shows an isometric view of the temperature distribution at 0.5 seconds into the simulation.

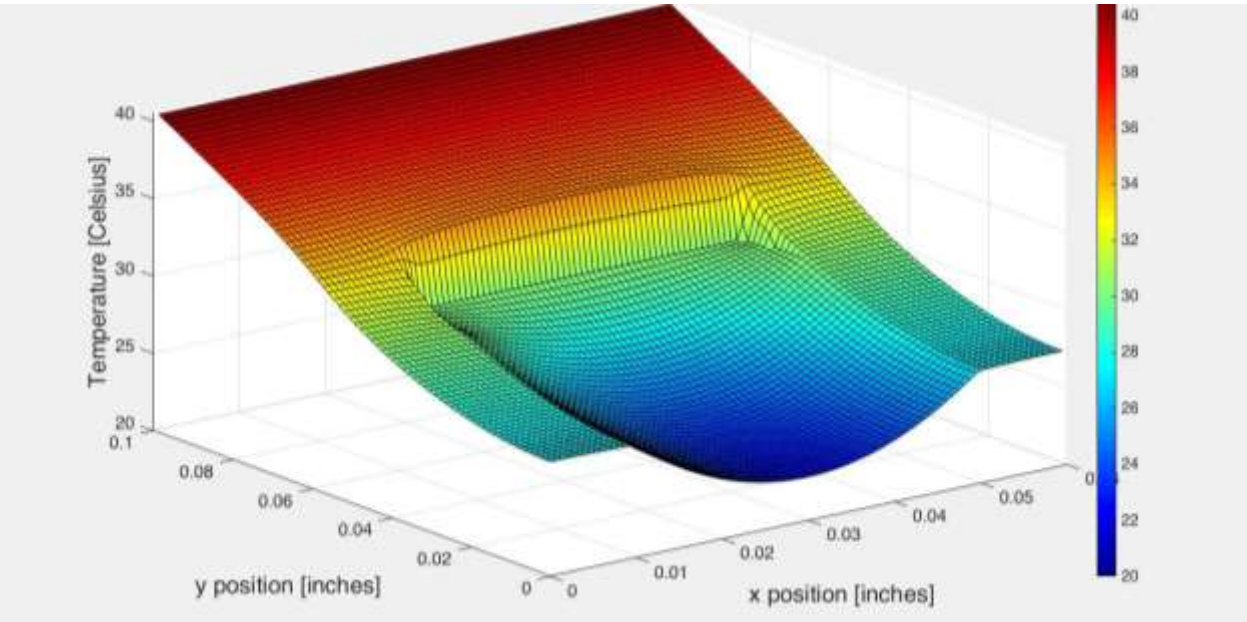

Figure 5. Isometric View of Fin Temperature Distribution

The boundary between the PCM and the fin material is clearly visible, as the heat coming from the far wall moves through the fins much quicker than through the PCM due to the fins higher conductivity. Figure 6, Figure 7, and Figure 8 below show a direct view of the distribution

of phase change throughout the PCM as time progresses through the simulation. As displayed in the plots, the red area represents the stainless-steel fin, dark blue is the solid PCM, yellow is the liquid PCM, and light blue is the transitioning PCM. The plots clearly show the progression of the plots as the PCM is changing phase; the single transition front that as to be expected from the simulation is apparent.

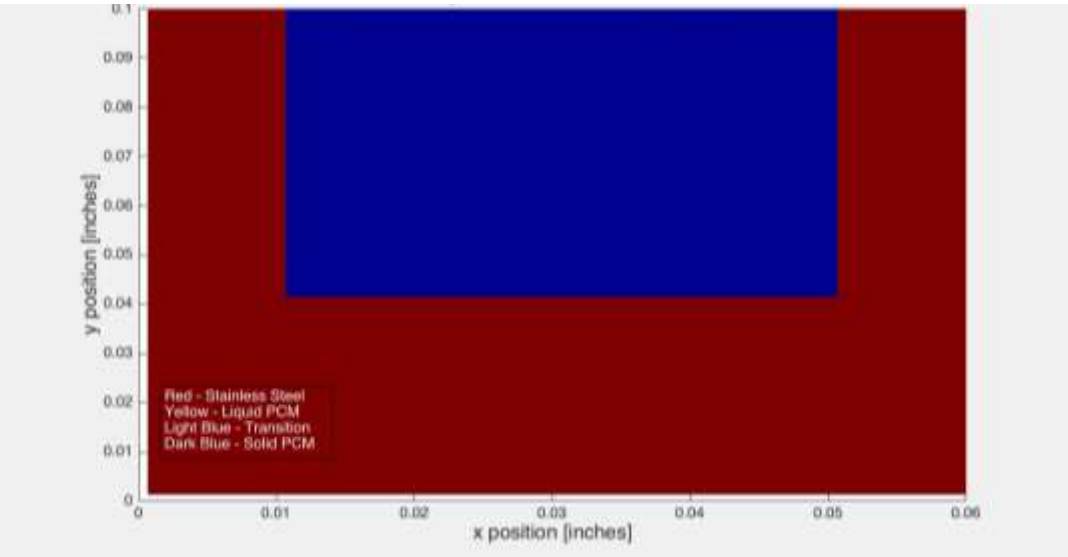

Figure 6. Fin State Distribution - 0 Seconds

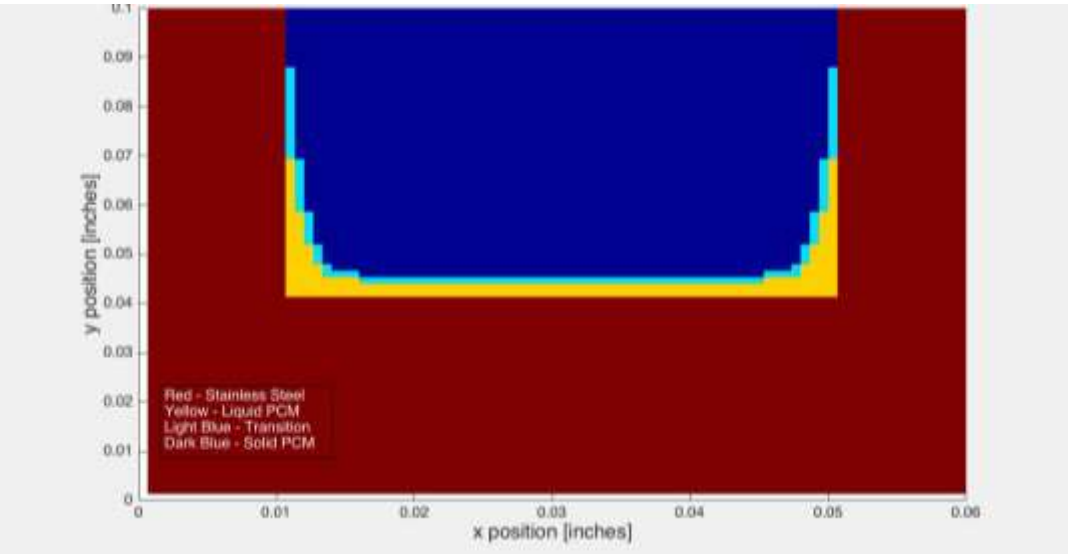

Figure 7. Fin State Distribution - 1 Second

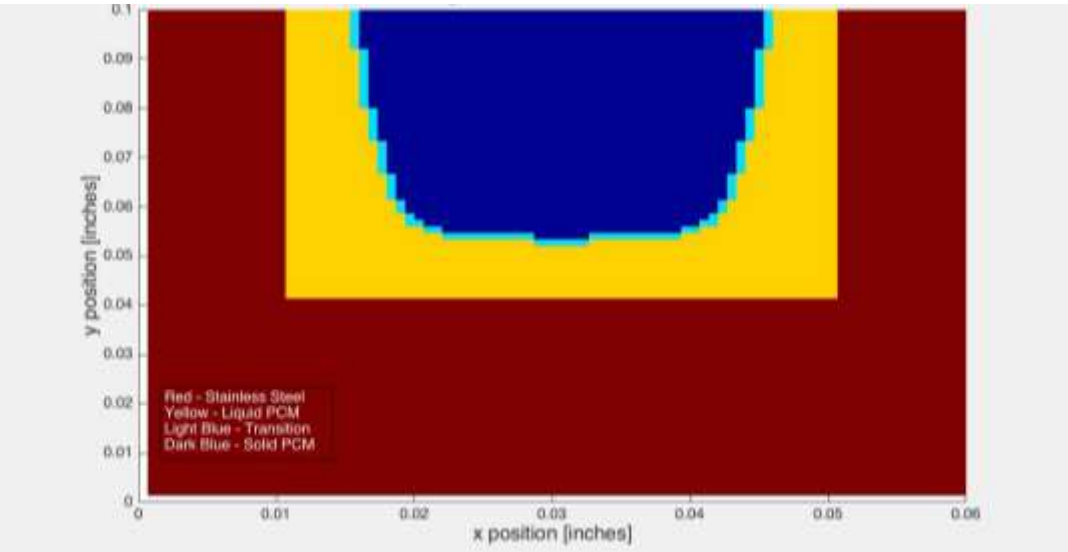

Figure 8. Fin State Distribution - 5 Seconds

The above simulation took 19.86 seconds to completely melt the PCM. This setup had a fin width of .02 inches, a fin height of 0.06 inches, and a PCM gap size of 0.04 inches. To optimize fin geometry, these values were varied in the simulation as described above in Section II. The full results from the geometry iteration process is tabulated within Table 2 in the appendix. The general trends of the study show that increasing fin spacing (or PCM gap) also increased the melt time/volume ratio. Increasing fin height also tends to increase this ratio, although with a much smaller impact than changing the fin spacing. Decreasing the fin width tends to decrease the time/volume ratio. These trends demonstrate that lowering each of these parameters causes the heat exchanger to be more effective at quickly transferring heat into the PCM, which is the desired result.

The geometry that produced the lowest melt time to volume ratio was with a fin width of 0.015 inches, a fin height of 0.05 inches, and a fin spacing of 0.03 inches. This was also the smallest fin geometry out of any that was tested, which leads to the speculation that smaller and smaller geometries lead to more effective fins. However, due to the relatively small number of

fin geometries that were tested, more study and simulations will need to be conducted before this assertion can be made from the created simulation.

Simulation Validation

With any sort of modeling it is important to validate the accuracy of the results. Because a single continuous body is being broken into multiple distinct elements, it must be confirmed that the elements it is broken into are sufficiently small enough to create an accurate model. With any simulation, it is expected that the as the number of nodes is increased, the simulation will converge to the correct answer. However, it is not feasible to simply run the simulation with an obscenely large number of nodes because the computer may not be capable of handling it or the run time will be longer than acceptable. Thus, validating the results of the simulation also serves to help find the balance between the accuracy and required run time of the model.

To do this, the simulation was run multiple times with various node densities and the results recorded in Table 1. Various simulation results were plotted against the number of nodes and it was shown that, for the nominal fin geometry, simulations results were insensitive to the number of nodes after approximately 1000 nodes.

Table 1. Simulation Validation Results

x nodes	y nodes	total nodes	Time Step	Time to Melt [s]	Average Power [W]	Run Time
2	3	6	0.0157688	19.7741	334.878	0.01
8	13	104	0.0006308	19.7615	346.780	1.00
15	25	375	0.0001577	19.8134	347.526	11.53
23	38	874	0.0000701	19.8205	347.052	57.84
26	43	1118	0.0000546	19.8257	346.187	94.97
30	50	1500	0.0000394	19.8406	347.727	177.00
35	58	2030	0.0000298	19.8368	347.263	318.13
38	63	2394	0.0000252	19.8394	346.872	464.67
45	75	3375	0.0000175	19.8513	347.764	1005.00

As the table shows, the Time to Melt and the Average Power were very consistent with their dependence on node density decreasing as the node count increased. However, it is hard to read this from a table so these results were plotted as well to show their convergence. The following figures show each of the three right most columns of the table plotted against the number of nodes used in the simulation.

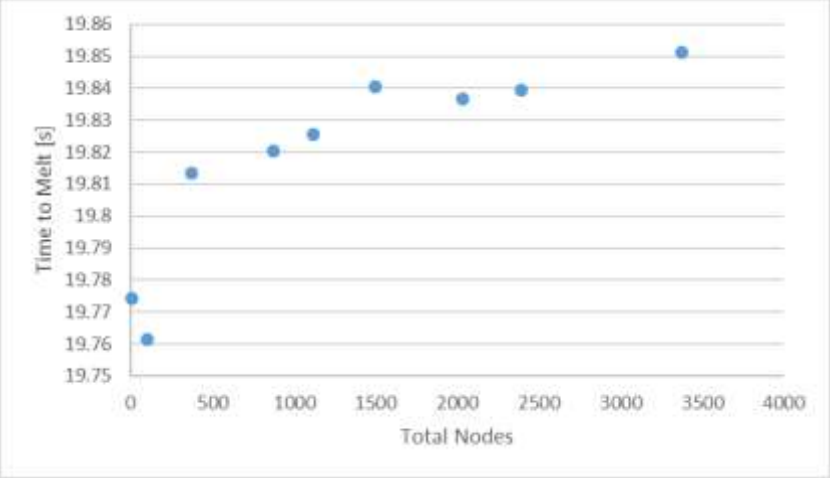

Figure 9. Time to Melt plotted against the Number of Nodes

Figure 9 shows the time to melt for converging to approximately 19.84 seconds. It is important to note the scale on this graph. The variations shown between data points that are within the convergance regaion are on the order of one or two hundredths of a second. This level of accuracy is more than enough for the scope of the simulation the team developed.

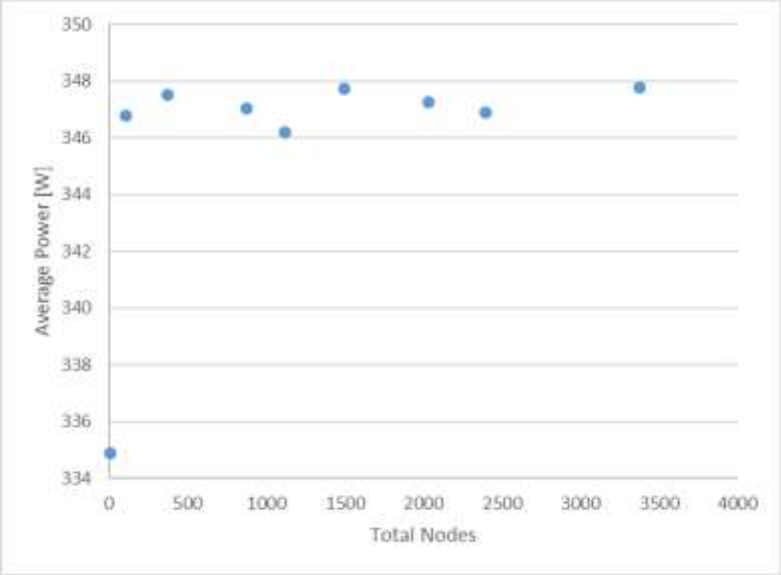

Figure 10. Average Power plotted against Number of Nodes

The average power converges even more clearly than the time to melt. Figure 10 shows the average power quickly converging to about 347 Watts with as few as 500 nodes. The way the data points continue to cluster around that line as the number of nodes was increased all the way to 3375 provides extra assurance that 347 Watts is the correct value. Clearly the average power was not as sensitive to the number of nodes as the time to melt was. Figure 11 shows the relationship between the amount of time taken to run the model and the number of nodes.

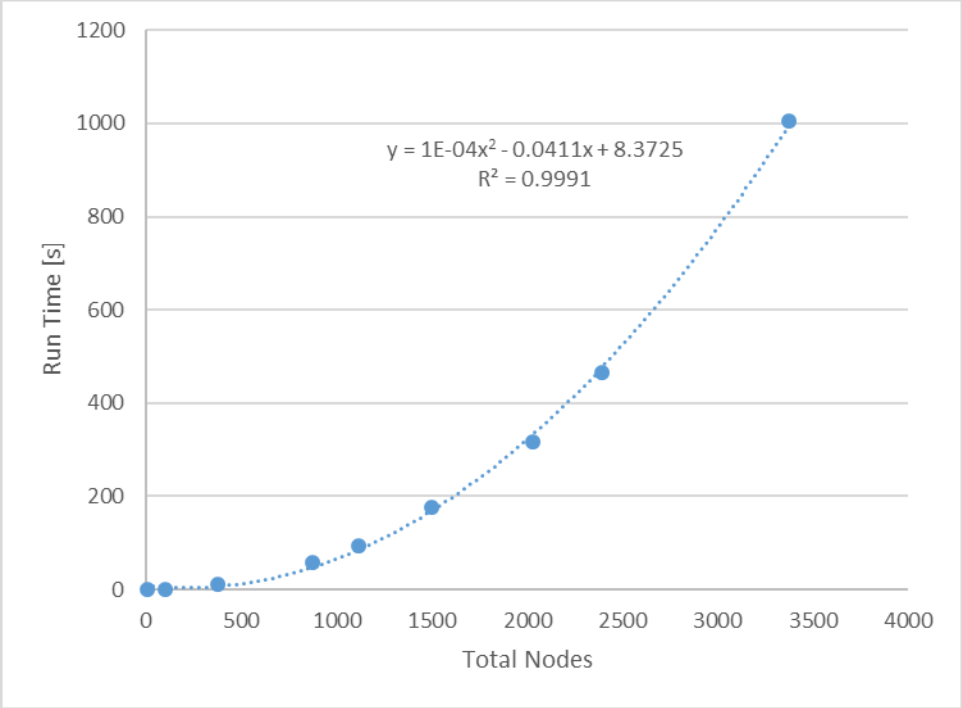

Figure 11. Simulation Run Time plotted against Number of Nodes

To keep all things equal, all the simulations of various node counts were run on the same computer to ensure that factors such as RAM and processing power were not confounding variables. As expected, as the number of nodes increases the time required to run the simulation increased. It is much more interesting to note that the trend almost perfectly fits a quadratic curve, and thus the simulations runs in $O(n^2)$ time. The runtime is due to the overall operation generally consisting of two, nested loops with constant-time (O(1)) operations.

From the table and the graphs, it has been shown that the maximum number of nodes the team tested is more than sufficient to accurately model the system. In fact, the node count could be reduced by as much as a factor of 2 to save on run time without compromising the accuracy by any appreciable amount. This is important because, as with any modeling, the user will want to find the best balance between quick run times and model accuracy.

SECTION IV

CONCLUSION

Using finite difference methods, a computational model was built which was capable of simulating heat transfer through phase change materials for the particular geometry of a flat plate with extended rectangular fins. This model was capable of utilizing temperature dependent properties to more accurately represent the behavior of the modeled materials. This simulation was used as a first step in determining an optimum fin geometry for use with a phase change material. A study was conducted which iterated through various fin geometries to determine the fin effectiveness in quickly melting the PCM, while accounting for the desire to prioritize higher volumes of PCM. The study concluded that smaller fin widths and smaller gaps between fins resulted in the lowest ratio of melting time to total PCM volume within a given model heat exchanger. This result intuitively makes sense because finned heat exchangers are known to generally be more effective as the number of fins increases because heat can more easily flow through the fins into the surrounding material. This result does not, however, provide a concrete optimal fin geometry, as smaller geometries continue giving better results.

After the creation of the computational model, validation methods were used to legitimize the results of the model. A node sensitivity study was used as the method of validating the model. The validation process clearly showed that increasing the number of nodes in the simulation caused the PCM melting time as well as the power into the system to converge. The convergence of the study shows that the designed model produces a stable solution.

Future work will include building a heat exchanger to both test phase change materials as well as verifying the accuracy of the computational model. The model has demonstrated the

importance of having smaller fins, so the heat exchanger plate will be made with the smallest fins that are feasible with available manufacturing techniques. In addition to this, further studies of the model will be conducted with larger ranges of fin geometry configurations to determine if any further conclusions about optimum fin geometries can be made.

REFERENCES

[1] Lewis, Roland Wynne, et al. The finite element method in heat transfer analysis. John Wiley & Sons, 1996.

[2] Reddy, Junuthula Narasimha. An Introduction to Nonlinear Finite Element Analysis: with applications to heat transfer, fluid mechanics, and solid mechanics. OUP Oxford, 2014.

[3] Hsiao, J. S. "An efficient algorithm for finite difference analyses of heat transfer with melting and solidification." Numerical Heat Transfer 8.6 (1985): 653666.

[4] Wilkes, J. O., and S. W. Churchill. "The finite-difference computation of natural convection in a rectangular enclosure." AIChE Journal 12.1 (1966): 161166.

APPENDIX

Table 2. Geometry Iteration Results

Fin Width [in]	Fin Height [in]	PCM gap [in]	Volume of PCM [in3]	Time to melt [s]	Time/Volume Ratio
0.015	0.05	0.03	0.6075	12.3263	20.29020576
0.015	0.05	0.04	0.66	17.2953	26.205
0.015	0.05	0.05	0.7	22.8876	32.69657143
0.015	0.05	0.06	0.735	28.1157	38.25265306
0.015	0.06	0.03	0.729	15.8114	21.68916324
0.015	0.06	0.04	0.792	22.8002	28.78813131
0.015	0.06	0.05	0.84	28.8655	34.36369048
0.015	0.06	0.06	0.882	35.6628	40.43401361
0.015	0.07	0.03	0.8505	18.5822	21.84855967
0.015	0.07	0.04	0.924	26.5579	28.74231602
0.015	0.07	0.05	0.98	33.3095	33.98928571
0.015	0.07	0.06	1.029	41.1019	39.94353741
0.02	0.05	0.03	0.5475	11.516	21.03378995
0.02	0.05	0.04	0.61	16.091	26.37868852
0.02	0.05	0.05	0.65	21.3266	32.81015385
0.02	0.05	0.06	0.69	26.2613	38.05985507
0.02	0.06	0.03	0.657	14.5446	22.13789954
0.02	0.06	0.04	0.732	19.8257	27.08428962
0.02	0.06	0.05	0.78	26.2311	33.62961538
0.02	0.06	0.06	0.828	32.3989	39.12910628
0.02	0.07	0.03	0.7665	16.9606	22.12733203
0.02	0.07	0.04	0.854	22.6961	26.57622951
0.02	0.07	0.05	0.91	29.8316	32.78197802
0.02	0.07	0.06	0.966	36.7128	38.00496894
0.025	0.05	0.03	0.495	10.6744	21.56444444
0.025	0.05	0.04	0.56	15.3444	27.40071429
0.025	0.05	0.05	0.6125	20.3538	33.23069388
0.025	0.05	0.06	0.645	25.6644	39.78976744
0.025	0.06	0.03	0.594	13.2322	22.27643098
0.025	0.06	0.04	0.672	18.6205	27.70907738
0.025	0.06	0.05	0.735	24.5983	33.46707483
0.025	0.06	0.06	0.774	31.3545	40.50968992
0.025	0.07	0.03	0.693	15.2805	22.04978355
0.025	0.07	0.04	0.784	21.1322	26.95433673
0.025	0.07	0.05	0.8575	27.6783	32.27790087
0.025	0.07	0.06	0.903	35.3104	39.103433